20th International Conference on Renewable Energies and Power Quality (ICREPQ'22)
Vigo (Spain), 27th to 29th July 2022
Renewable Energy and Power Quality Journal (RE&PQJ)
ISSN 2172-038 X, Volume No.20, September 2022

Stability study of AC grid-connected quasi-Z-source inverter-based photovoltaic power systems

L. Sainz[1], Ll. Monjo[2], F. Jurado[3]

[1] Department of Electrical Engineering
E.T.S.E.I.B., UPC
Av. Diagonal 647, 08028 Barcelona (Spain)
Phone/Fax number: +0034 93 4011759, e-mail: luis.sainz@upc.edu

[2] Department of Electrical Engineering
E.P.S.E.V.G., UPC
Victor Balaguer s/n, 08800 Vilanova i la Geltrú, Spain
Phone/Fax number: +0034 93 4010746, e-mail: lluis.monjo@upc.edu

[2] Department of Electrical Engineering
University of Jaén
23700 EPS Linares, Jaén, Spain
Phone/Fax number: +0034 953 64 85 18, e-mail: fjurado@ujaen.es

Abstract. The presence of photovoltaic power systems is currently increasing as green power sources, and quasi-Z-source inverters are commonly used to connect them to AC grids. However, stability concerns can appear due to inverters. Several studies address these concerns but they are not completely solved yet. This paper contributes with a simulation study about stability of AC grid-connected quasi-Z-source inverter-based photovoltaic power systems. The study is based on the PSCAD/EMTDC model of these systems and analyzes the influence of system parameters on subsynchronous and harmonic instabilities. Several solutions to improve these instabilities are discussed.

Key words. Photovoltaic systems, quasi-Z-source inverters, stability, small-signal model, PSCAD/EMTDC model

1. Introduction

Photovoltaic (PV) power systems are currently used as sustainable power sources [1] – [3]. These systems are formed by single- or two-step converters. The latter topology is more common, [4], [5], but the former is becoming increasingly used. Among this type, we find quasi-Z-source inverters (qZSIs) [6] – [9]. These inverters have a semiconductor, capacitor and inductor DC circuit with buck-boost options [6], [10] – [15]

AC grid-connected qZSI-based PV power systems can have stability problems due to the interaction between converters and the AC grid. Several authors analyze this concern in the two-step converter configuration, concluding that changes in control, temperature and irradiance can worsen system stability [3], [10], [11], [16] – [19]. The qZSI dynamics [6] – [8], [10] – [12], [15] and qZSI-based PV power system stability [18] – [24] are also investigated, but AC grid-connected qZSI-based PV power system stability has not been completely analyzed yet. Various AC-side admittance-based matrix approaches are proposed to assess multi-terminal AC grid-connected converter stability in the s-domain (e.g., eigenvalue analysis [25] – [27]), and in the frequency domain (e.g., Generalized Nyquist Criterion [28] – [33]).

This paper studies AC grid-connected qZSI-based PV power system stability using the PSCAD/EMTDC model, and several simulations are made with it. The causes of instability and possible solutions are discussed.

2. PSCAD/EMTDC model of AC grid-connected qZSI-based PV power systems

Stability of the AC grid-connected qZSI-based PV power system in Fig. 1 is studied from its PSCAD/EMTDC implementation.

The qZSI-based PV power system is connected to a filter capacitor C_f and an AC grid. It has a PV plant (formed by N_p parallel strings of N_s PV cells in series, the capacitor C_p and the DC cable resistance R_c [2], [4]) feeding the qZSI [6] – [9], which boosts the output DC voltage at the VSI input. The PV plant is modeled with its equivalent circuit derived from the linearization of the I-V curve of the PV panel around the MPP [4], [23], [24]. The AC grid is characterized by the short-circuit inductance L_s and the supply AC voltage e_s to be able to represent the connection of the qZSI-based PV power system to the weak parts of the grid.

The controls of the qZSI-based PV power system, i.e., MPPT, PV voltage, current and duty cycle controls, are also shown in Fig. 1. Maximum power of the PV plant is obtained by the MPPT algorithm [4], [23] and voltage control of the PV plant. The current control of the VSI imposes the power delivered from the PV plant to the AC

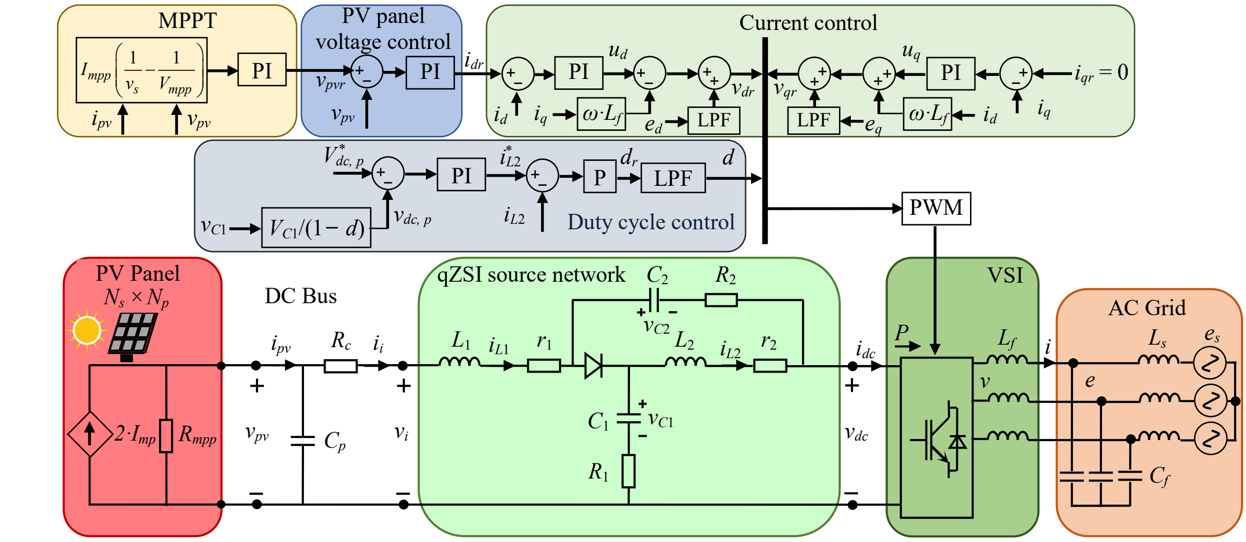

Fig. 1. AC grid-connected qZSI-based PV power system.

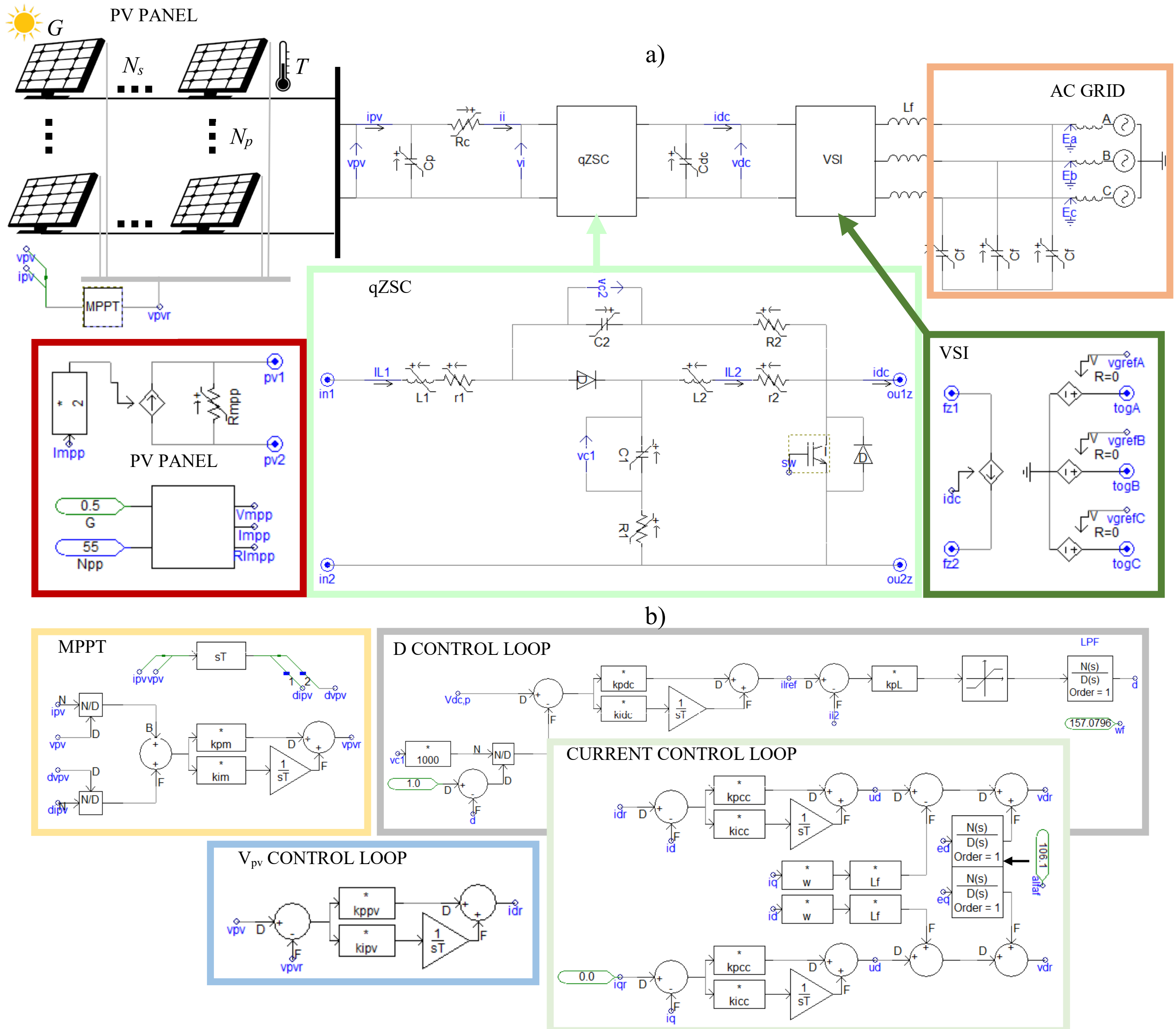

Fig. 2. PSCAD/EMTDC model of the AC grid-connected qZSI-based PV power system: (a) power circuit; (b) control circuit.

grid [6]. The qZSI duty cycle control adjusts the DC peak voltage at the VSI terminals [6], [12].

The PSCAD/EMTDC implementation of the AC grid-connected qZSI-based PV power system is shown in Fig. 2. The PSCAD/EMTDC model is formed by the power modules of the qZSI-based PV power system and AC grid (see Fig. 2(a)), and the four controls in the qZSI-based PV power system (see Fig. 2(b)). The components

Table I.- qZSI-based PV Power System Data
(U_N = 1 kV DC, P_N = 0.1 MW)

	Parameters	Data
PV cell [2]	G, T	0.5 Sun, 25ºC
PV installation	N_p, N_s	55, 42
	R_c, C_p	0.0667Ω, 10 mF
qZSI source network	$L_1 = L_2$, $r_1 = r_2$	0.3 mH, 0.011 Ω
	$C_1 = C_2$, $R_1 = R_2$	3 mF, 0.006 Ω
VSC	L_f	0.4 mH
MPPT control	$k^m{}_p$, $k^m{}_i$	0.01 Ω, 0.5 Ω/s
PV control	$k^{pv}{}_p$, $k^{pv}{}_i$	1.8 Ω^{-1}, 75 Ω^{-1}/s
CC control	$k^{cc}{}_p$, $k^{cc}{}_i$	0.424 Ω^{-1}, 150 Ω^{-1}/s
	$\alpha_f = 0.1 \cdot k^{cc}{}_p/L_f$	106.1 rad/s
D control (D = 0.06)	$V^*{}_{dc,\,p}$	800 V
	$k^{dc}{}_p$, $k^{dc}{}_i$	0.016 V^{-1}, 75 V^{-1}/s
	$k^L{}_p$	10^{-4} A^{-1}
NOTE:	All variables are defined in Figs. 1 and 2	

of the PSCAD/EMTDC model in Fig. 2 can be identified with the elements of the qZSI-based PV power system in Fig. 1 by the colour code and the labels. All the components used to build the PSCAD/EMTDC model are from the PSCAD library.

PSCAD/EMTDC time domain simulations with the circuit in Fig. 2 make it possible to check the influence of circuit parameters on the dynamic behaviour of AC grid-connected qZSI-based PV power systems, assess system stability and test solutions for improving stability issues. These simulations were carried out using 2 μs time step. In order to increase simulation efficiency, a snapshot file was created when the circuit reached its steady-state operation point, and this file was used in subsequent simulations in order not to have to simulate the initial transient every time and speed up the analysis.

3. Frequency domain response of the qZSI-based PV power system

The frequency response of the pn-sequence domain admittance transfer matrix terms of the qZSI-based PV power system allows the influence of this system on AC grid-connected qZSI-based PV power system stability to be analyzed. This frequency response can be obtained from PSCAD/EMTDC simulations made with the model proposed in the previous Section. Based on these simulations, a qZSI-based PV power system with a PV panel supplying a 0.1 MW 1 kV DC PV power system connected to a strong 400 V AC grid is studied (see data in Table I). It must be note that a strong grid is only made for the validation of the model while a weak grid is considered in one of the examples of the next Section.

The pn-sequence domain admittance transfer matrix terms are characterized by two independent PSCAD/EMTDC simulation tests, where frequency domain analysis is performed with the FFT of the involved voltages and currents [35]. In the tests, a series small-signal harmonic perturbation of p- and n-sequence voltages, $\mathbf{U_p}$ and $\mathbf{U_n}$, of frequencies f_p and f_n is applied to the qZSI-based PV power system in Fig. 2. Because of these voltages, the

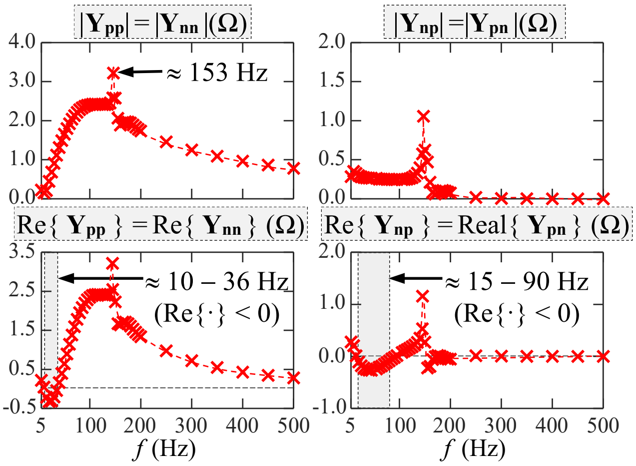

Fig. 3. PSCAD frequency response of the pn-sequence domain admittance transfer matrix of qZSI-based PV power systems.

qZSI-based PV power system consumes p- and n-sequence currents, $\mathbf{I_p}$ and $\mathbf{I_n}$, of frequencies f_p and $f_n = f_p - 2f_1$ (mirror frequency) in the p-sequence test with $\mathbf{U_p}$, and frequencies $f_p = f_n + 2f_1$ (mirror frequency) and f_n in the n-sequence test with $\mathbf{U_n}$. Finally, the pn-sequence domain admittance transfer matrix terms of dq-complex domain frequency $f = f_p - f_1$ (in the p-sequence domain test with $\mathbf{U_p}$) and $f = f_n + f_1$ (in the n-sequence domain test with $\mathbf{U_n}$) are calculated as follows:

$$\mathbf{Y_{pp}} = \frac{\mathbf{I_p}}{\mathbf{U_p}} \qquad \mathbf{Y_{np}} = \frac{\mathbf{I_n}}{\mathbf{U_p}}$$
$$\mathbf{Y_{pn}} = \frac{\mathbf{I_p}}{\mathbf{U_n}} \qquad \mathbf{Y_{nn}} = \frac{\mathbf{I_n}}{\mathbf{U_n}}. \tag{1}$$

The frequency response of the pn-sequence domain admittances is shown in Fig. 3. This response reveals two important issues of qZSI-based PV power systems (see Section 4):

- They have a resonance frequency (e.g., at 153 Hz in Fig. 3) which could cause harmonic oscillatory instabilities of the qZSI-based PV power system at this frequency if this resonance is undamped [24].
- They have a negative-damping region (see Fig. 3) which could lead to subsynchronous resonance instabilities of AC grid-connected qZSI-based PV power systems if there are system resonances in this region.

4. Examples

Stability of AC grid-connected qZSI-based PV power systems is analyzed by PSCAD/EMTDC time domain simulations with the model in Section 2 and the data in Table I. The network with a 0.1 MW 1 kV DC qZSI-based PV power system in Fig. 1 is connected to a VSC filter capacitor C_f = 100 μF and a 400 V 50 Hz AC grid with a short-circuit ratio SCR equal to 20. The examples show stability problems in AC grid-connected qZSI-based PV power systems. Three cases are studied

- Case #1: this is the stable reference case, which corresponds to the PV power system steady-state operating point with $G = 0.4$ Sun, $T = 25^{\circ}$ C and SCR equal to 20.

- Case #2: the irradiance level G is stepped up from 0.4 to 0.8 Sun to study its influence on stability.
- Case #3: the SCR is stepped down from 20 to 3 to study instabilities due to weak AC grids. Note that this is an interesting example because the location of the PV plants often forces the VSI to be interconnected in the weak parts of the grid.

System stability in the above cases is studied with the PSCAD/EMTDC simulations in Fig. 4. The AC grid-connected qZSI-based PV power system is stable in Case #1 but becomes unstable when the parameter G reaches a value of 0.8 at 1.8 s and the parameter SCR decreases to 3 at 1 s. The frequency of the unstable oscillations captured by the PSCAD/EMTDC simulations is $f_{osc} \approx 155$ Hz when G is stepped up (Case #2) and $f_{osc} \approx 35$ Hz when SCR is stepped down (Case #3). In Case #2, the AC grid-connected qZSI-based PV power system has a harmonic instability because the parallel resonance of the qZSI-based PV power system in Fig. 3 is undamped [24]. In Case #3, the AC grid-connected qZSI-based PV power system has a subsynchronous instability due to the interaction between the weak AC grid and the negative-damping region of the qZSI-based PV power system at subsynchronous frequencies (see Fig. 3).

The harmonic instability in Case #2 can be improved by increasing the DC-link peak voltage $V_{dc,p}$ because it damps the qZSI-based PV power system resonance in Fig. 3 [23], [24], restoring AC grid-connected qZSI-based PV power system stability. This is verified in Fig. 4, where the step up of the DC-link peak voltage $V_{dc,p}$ from 800 V to 1000 V at 2.75 s enables system stability recovery. The subsynchronous instability in Case #3 can be improved by decreasing the bandwidth α_f of the current control feedforward filter (see Figs. 1 and 2) because this reduces the negative-damping region of the qZSI-based PV power system admittances in Fig. 3 [23], [24], and the harmonic resonance due to the weak grid is damped. This is verified in Fig. 4, where the step down of the bandwidth α_f from 106.1 rad/s to 95.5 rad/s at 1.2 s enables system stability recovery.

4. Conclusion

This paper studies subsynchronous and harmonic instabilities of AC grid-connected quasi-Z-based PV power systems by PSCAD/EMTP simulation. The PSCAD/EMTP model of the AC grid-connected quasi-Z-based PV power system is proposed and several examples are developed to study the origin of and possible solutions to instabilities. It is concluded that (i) the increase of irradiance level in the PV panels can lead to harmonic instabilities due to qZSI-based PV power system instability; (ii) the decrease of the SCR can lead to subsynchronous instabilities due to the interaction between the weak grid and the qZSI-based PV power system. The former is mitigated by increasing the DC-link peak voltage and the latter is improved by decreasing the bandwidth of the current control feedforward filter.

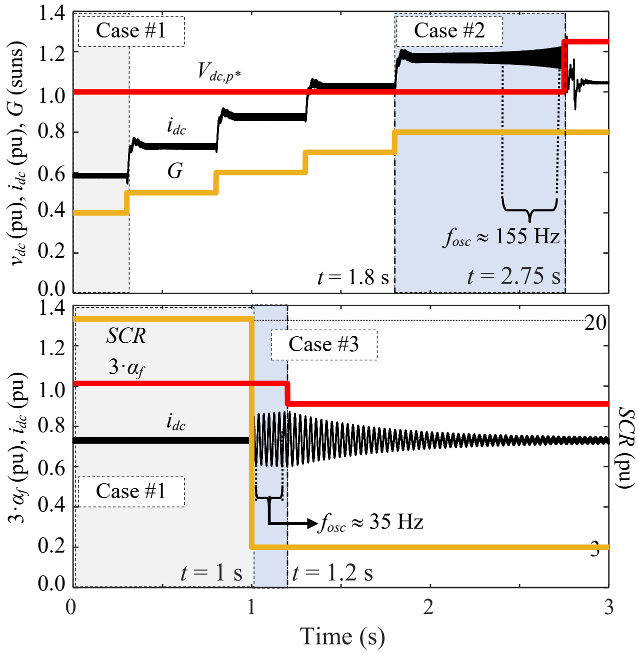

Fig. 4. PSCAD/EMTDC simulations ($S_B = 0.1$ MW, $U_B = 800$ V, $f_B = 50$ Hz).

Acknowledgement

This work was supported in part by the Ministerio de Ciencia, Innovación y Universidades under Grant RTI2018-095720-B-C33.

References

[1] Q. Fu et al., “Microgrid generation capacity design with renewables and energy storage addressing power quality and surety”, IEEE Trans. on Smart Grid (2012). Vol. 3, no. 4, pp. 2019–2027.

[2] G. Walker, “Evaluating MPPT converter topologies using a Matlab PV Model”, Journal of Electrical and Electronics Engineering (2001). Vol. 21, no. 1, pp. 49–55.

[3] S. Liu, P. X. Liu, X. Wang, “Stochastic Small-Signal Stability Analysis of Grid-Connected Photovoltaic Systems”, IEEE Trans. on Industrial Electronics (2016). Vol. 63, no. 2, pp. 1027–1038.

[4] M. Pokharel, A. Ghosh, C. N. Man Ho, “Small-Signal Modelling and Design Validation of PV-Controllers With INC-MPPT Using CHIL”, IEEE Trans. Energy Conv. (2019). Vol. 34, no. 1, pp. 361–370.

[5] Y. Liu, B. Ge, H. Abu-Rub, F. Z. Peng, “An effective control method for quasi-Z-source cascade multilevel inverter-based grid-tie single-phase photovoltaic power system”, IEEE Trans. Ind. Informatics (2014). Vol. 10, no. 1, pp. 399–407.

[6] Y. Liu, H. Abu-Rub, B. Ge, F. Blaabjerg, O. Ellaban, P. Chiang, Impedance source power electronic converters, John Wiley and Sons, IEEE Press, Chichester, West Sussex, UK (2016).

[7] Y. P. Siwakoti, F. Z. Peng, F. Blaabjerg, P. C. Loh, G. E. Town, “Impedance-source networks for electric power conversion. Part I: A topological review”, IEEE Transactions on Power Electronics (2015). Vol. 30, no. 2, pp. 699–716.

[8] Y. P. Siwakoti, F. Z. Peng, F. Blaabjerg, P. C. Loh, G. E. Town, S. Yang, “Impedance-source networks for electric power conversion. Part II: Review of control and modulation techniques”, IEEE Transactions on Power Electronics (2015). Vol. 30, no. 4, pp. 1887–1906.

[9] O. Husev, F. Blaabjerg, C. Roncero-Clemente, E. Romero-Cadaval, D. Vinnikov, Y. Siwatoki, R. Strzelecki, "Comparison of impedance-source networks for two and multilevel buck–boost inverter applications", IEEE Transactions on Power Electronics (2016). Vol. 31, no. 11, pp. 7564–7579.
[10] J. Liu, J. Hu, L. Xu, "Dynamic modeling and analysis of Z-source converter-derivation of AC small signal model and design-oriented analysis", IEEE Trans. Power Electron. (2007). Vol. 22, no. 5, pp. 1786–1796.
[11] Y. Li, J. Anderson, F. Z. Peng, D. Liu, "Quasi-Z-Source Inverter for Photovoltaic Power Generation Systems", in Proc. 2009 Twenty-Fourth Annual IEEE Applied Power Electronics Conference and Exposition, Washington, DC, USA, 2009, pp. 918–924.
[12] Y. Liu, B. Ge, F. J. T. E. Ferreira, A. T. de Almeida, H. Abu-Rub, "Modeling and SVPWM control of quasi-Z-source inverter", in Proc. 11th International Conference on Electrical Power Quality and Utilisation (EPQU), Lisbon, Portugal, 2011, pp.1–7.
[13] J. Anderson, F. Z. Peng, "Four quasi-Z-Source inverters", in Proc. IEEE Power Electronics Specialists Conference, Rhodes, Greece, 2008, pp. 2743–2749.
[14] C. Roncero-Clemente, E. Romero-Cadaval, O. Husev, D. Vinnikov, S. Stepenko, "Simulation of Grid Connected Three-Level Neutral-Point-Clamped qZS Inverter using PSCAD", Electrical, Control and Communication Engineering (2013). Vol. 2, no. 1, pp. 14–20.
[15] O. Husev, C. Roncero-Clemente, S. Stepenko, D. Vinnikov, E. Romero-Cadaval, "CCM operation analysis of the single-phase three-level quasi-Z-source inverter", in Proc. 15th International Power Electronics and Motion Control Conference (EPE/PEMC), Novi Sad, 2012, pp. DS1b.21-1-DS1b.21–6.
[16] Y. Tan, D. Kirschen, N. Jenkins, "A model of PV generation suitable for stability analysis", IEEE Trans. on Energy Conversion (2004). Vol. 19, no. 4, pp. 748–755.
[17] Y. Xue, M. Manjrekar, C. Lin, M. Tamayo, J. Jiang, "Voltage stability and sensitivity analysis of grid-connected photovoltaic systems", in Proc. IEEE PES Gen. Meet., Detroit, MI, USA, Jul. 2011, pp. 1–7.
[18] V. Castiglia, R. Miceli, F. Blaabjerg, Y. Yang, "Small-Signal Modeling and Experimental Validation of the Three-phase Quasi-Z-Source Inverter", in Proc. IEEE 21st Workshop on Control and Modeling for Power Electronics (COMPEL), Aalborg, Denmark, 2020, pp. 1–8.
[19] S. Stepenko, O. Husev, D. Vinnikov, C. Roncero-Clemente, S. Pires Pimentel, E. Santasheva, "Experimental Comparison of Two-Level Full-SiC and Three-Level Si–SiC Quasi-Z-Source Inverters for PV Applications", Energies (2019). Vol. 12, no. 13, pp. 2509.
[20] Z. Liang, S. Hu, H. Yang, X. He, "Synthesis and Design of the AC Current Controller and Impedance Network for the Quasi-Z-Source Converter", IEEE Transactions on Industrial Electronics (2018). Vol. 65, no. 10, pp. 8287–8296.
[21] W. Liu, Y. Yang, T. Kerekes, E. Liivik, F. Blaabjerg, "Impedance Network Impact on the Controller Design of the qZSI for PV Applications", in Proc. IEEE 21st Workshop on Control and Modeling for Power Electronics (COMPEL), Aalborg, Denmark, 2020, pp. 1–6
[22] L. Oliveira-Assis, E. P. P. Soares-Ramos, R. Sarrias-Mena, P. García-Triviño, L. M. Fernández-Ramírez, "Large-Scale Grid Connected Quasi-Z-Source Inverter-Based PV Power Plant", in Proc. IEEE International Conference on Environment and Electrical Engineering and IEEE Industrial and Commercial Power Systems Europe (EEEIC / I&CPS Europe), Madrid, Spain, 2020, pp. 1–6.
[23] Ll. Monjo, L. Sainz, J. J. Mesas, J. Pedra, "Quasi-Z-Source Inverter-Based Photovoltaic Power System Modeling for Grid Stability Studies", Energies (2021). Vol. 14, no. 2, pp. 508.
[24] Ll. Monjo, L. Sainz, J. J. Mesas, J. Pedra, "State-Space Model of Quasi-Z-Source Inverter-PV Systems for Transient Dynamics Studies and Network Stability Assessment", Energies (2021). Vol. 14, no. 2, pp. 4150.
[25] E. Ebrahimzadeh, F. Blaabjerg, X. Wang, C. L. Bak, "Harmonic stability and resonance analysis in large PMSG-based wind power plants", IEEE Transactions on Sustainable Energy (2018). Vol. 9, no. 1, pp. 12–23.
[26] Y. Zhan, X. Xie, H. Liu, H. Liu, Y. Li, "Frequency-domain modal analysis of the oscillatory stability of power systems with high-penetration renewables" , IEEE Transactions on Sustainable Energy (2019). Vol. 10, no. 3, pp. 1534–1543.
[27] F. Xing, Z. Xu, Z. Zhang, Y. Dan, Y. Zhu, "Resonance Stability Analysis of Large-Scale Wind Power Bases with Type-IV Wind Generators", Energies (2020). Vol. 13, no. 19, p. 5220. Available online: https://www.mdpi.com/1996-1073/13/19/5220.
[28] X. Wang, F. Blaabjerg, W. Wu, "Modeling and Analysis of Harmonic Stability in an AC Power-Electronics-Based Power System", IEEE Trans-actions on Power Electronics (2014). Vol. 29, no. 12, pp. 6421–6432.
[29] J. Pedra, L. Sainz, L. Monjo, "Three-Port Small Signal Admittance-Based Model of VSCs for Studies of Multi-terminal HVDC Hybrid AC/DC Transmission Grids", IEEE Transactions on Power Systems (2021). Vol. 36, no. 1, pp. 732–743.
[30] Y. Li, Z. Shuai, X. Liu, Y. Chen, Z. Li, Y. Hong, Z. J. Shen, "Stability Analysis and Location Optimization Method for Multiconverter Power Systems Based on Nodal Admittance Matrix", IEEE Journal of Emerging and Selected Topics in Power Electronics (2021). Vol. 9, no. 1, pp. 529–538.
[31] H. Liu, X. Xie, W. Liu, "An oscillatory stability criterion based on the unified dq-frame impedance network model for power systems with high-penetration renewables", IEEE Trans. on Power Syst. (2018). Vol. 33, no. 3, pp. 3472–3485.
[32] H. Liu, X. Xie, "Impedance Network Modeling and Quantitative Stability Analysis of Sub-/Super-Synchronous Oscillations for Large-Scale Wind Power Systems", IEEE Access (2018). Vol. 6, pp. 34431–34438, doi: 10.1109/ACCESS.2018.2849830.
[33] E. Ebrahimzadeh, F. Blaabjerg, X. Wang, C. L. Bak, "Harmonic stability and resonance analysis in large PMSG-based wind power plants", IEEE Trans. on Sustainable Energy (2018). Vol. 9, no. 1, pp. 12–23.